Yamaguchi et al., http://www.jcb.org/cgi/content/full/jcb.201104057/DC1

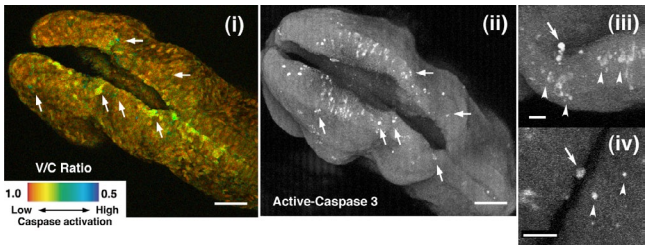

Figure S1. **The decrease in V/C was correlated with caspase activation in vivo.** SCAT3 transgenic embryos at E8.75 were dissected from the uterus and immediately immersed in fixative. After a short fixation, their images were captured by confocal microscopy to measure the V/C (i). The embryos were then processed for immunostaining with an anti–active caspase-3 antibody, and pictures were taken of the staining (ii). Later images were taken of the same embryo for comparison between i and ii. Some cells exhibiting a lower V/C (i) were also positive for anti–active caspase-3 immunostaining (ii), indicated by arrows. (iii and iv) Cells positive for active caspase-3 immunostaining in the MHNP at E8.75. Arrows indicate D-type apoptotic cells detaching from the neural ridge. Arrowheads indicate C-type apoptotic cells undergoing shrinkage and fragmentation. Bars: (i and ii) 100 µm; (iii and iv) 25 µm.

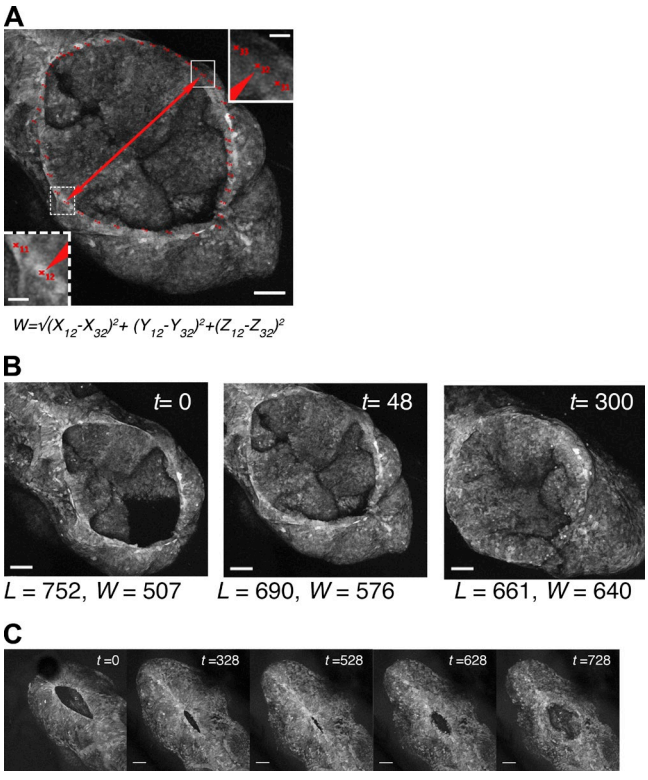

Figure S2. **Exencephaly as a possible consequence of delayed closure.** (A) Measurement of the width (*W*) of the MHNP from 3D datasets. The circumference of MHNP was tracked by marking the edges (boundary between the neuroectoderm and surface ectoderm) of the MHNP in the 3D data. Their coordinate values were used to calculate *W*, and two points marking the widest ventricular regions of r2 were identified. Bar, 100 µm. (insets) In this picture, the values of points 12 and 32 were used as shown by a red arrow. Bars, 25 µm. (B) Live imaging of the exencephalic brain of an *apaf-1*$^{-/-}$ embryo (somite 20). NTC failure had occurred before the culture began. During imaging, the MHNP length decreased (from 752 to 661 µm), but its width increased (from 507 to 640 µm), implying the presence of forces incompatible with closure, probably caused by the lateral expansion of ventricles in the embryonic brain. Length of MHNP and width of MHNP at r2 are shown in micrometers. (C) Reopening of the hindbrain neuropore in *apaf-1*$^{-/-}$ embryos expressing SCAT3. Time-lapse imaging of closures I and II in the hindbrain of an *apaf-1*$^{-/-}$ embryo. Progressive closures I and II suddenly stopped, and the midline began to reopen, despite the embryo still being alive, as judged from the strong heartbeat. (B and C) *t* is indicated in minutes. Bars, 100 µm.

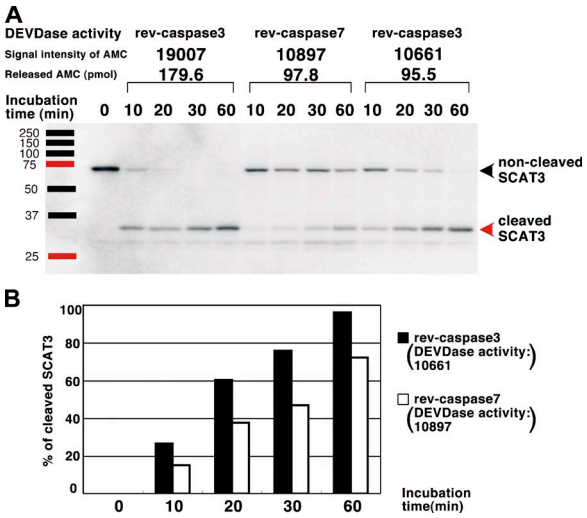

Figure S3. **Differential efficiency of SCAT3 cleavage by caspase-3 and caspase-7.** (A) In vitro cleavage assay of SCAT3 by reverse caspase-3 (rev-caspase3) and reverse caspase-7 (rev-caspase7). At the similar DEVDase activities, reverse caspase-3 had a higher efficiency of SCAT3 cleavage than reverse caspase-7. Enzymatic activity was measured by the amount of 7-amino-4-methylcoumarin (AMC) which is released by cleavage of DEVD-MCA. Molecular mass is indicated in kilodaltons. (B) Quantification of the ratio of cleaved SCAT3 bands/total amounts of SCAT3 (sum of cleaved and noncleaved SCAT3 bands) at the similar DEVDase activity in A. Experiments were performed twice independently, and a representative result is presented here.

Video 1. **Live imaging of the zipping process in rostral closure I.** As shown in Fig. 2 E, a *SCAT3*$^{tg/+}$ embryo undergoing only closure I was observed under a fast-scanning confocal microscope. ECFP images are shown. Zipping was clearly visualized (blue line). Live imaging was performed on an inverted confocal microscope (TCS SP5). Frames were taken at intervals of 4 min for 12 h.

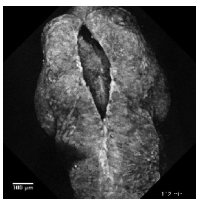

Video 2. **Live imaging of the sealing MHNP by closures I and II.** Time-lapse video of a *SCAT3*$^{tg/+}$ embryo undergoing MHNP closure, as shown in Fig. 2 F. ECFP images are shown. MHNP was sealed by closures I and II. Live imaging was performed on an inverted confocal microscope (TCS SP5). Frames were taken at intervals of 4 min for 14 h.

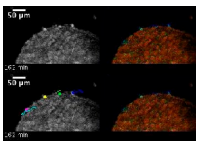

Video 3. **Concomitant occurrence of D-type apoptotic cells during neural plate morphogenesis.** Time-lapse video of apoptosis during flipping of the neural ridge and bending of the neural plate, as shown in Fig. 3 C. The neural ridge of the midbrain–hindbrain of a *SCAT3*$^{tg/+}$ embryo undergoing only closure I was observed. D-type apoptotic cells first appeared and continuously danced at the boundary ridge between the neuroectoderm (neural plate) and surface ectoderm. Some of them tumbled down the neural plate, as shown by tracking in the ECFP image (bottom left). As its ridge flipped and the neural plate bent, apoptotic cells were abundantly observed beneath the flipped neural ridge (the presumed dorsolateral hinge point, shown by arrows in the last frame of the video). Caspase activation is indicated by the V/C (1.0–0.5) using pseudocolor. Live imaging was performed on an inverted confocal microscope (TCS SP5). Frames were taken at intervals of 6 min for 12 h.

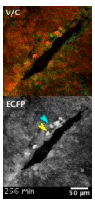

Video 4. **Occurrence of C-type apoptotic cells before and during the midline fusion.** Time-lapse video of apoptosis before and during the midline fusion in MHNP closure, as shown in Fig. 3 E. Boundary cells underwent C-type apoptosis (judged by immediate cell fragmentation after caspase activation) before and during sealing of the midline. Some of the cells undergoing C-type apoptosis in the midline were marked first by yellow arrowheads and after caspase activation by cyan in the ECFP image (bottom). Caspase activation is indicated by the V/C (1.0–0.5) using pseudocolor (top). Live imaging was performed on an inverted confocal microscope (TCS SP5). Frames were taken at intervals of 4 min for 12 h.

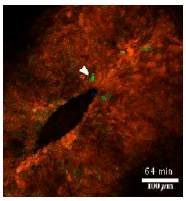

Video 5. **Occurrence of C-type apoptotic cells after the midline fusion.** Time-lapse video of apoptosis during and after the midline fusion in MHNP closure, as shown in Fig. 3 F. C-type apoptosis abundantly occurred after sealing of the midline by closure II. Some of the cells undergoing C-type apoptosis in the midline are shown by white arrowheads. Caspase activation is indicated by the V/C (1.0–0.5) using pseudocolor. Live imaging was performed on an inverted confocal microscope (TCS SP5). Frames were taken at intervals of 4 min for 12 h.

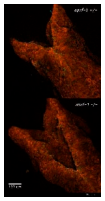

Video 6. **Comparison of the neural plate morphogenesis between *apaf-1*$^{+/-}$ and *apaf-1*$^{-/-}$ embryos by the live-imaging analysis of SCAT3.** In the *apaf-1*$^{+/-}$ embryo, flipping of the neural ridges occurred smoothly and concomitantly with apoptosis in that region (top), as shown in Fig. 6 A. In *apaf-1*$^{-/-}$ embryos, both the flipping and the apoptosis were severely reduced (bottom). In addition, the neural ridges in *apaf-1*$^{-/-}$ embryos exhibited repeated squeezing motions, but they failed to complete the apposition and zipping. Caspase activation is indicated by the V/C (1.0–0.5) using pseudocolor. Live imaging was performed on an inverted confocal microscope (TCS SP5). Frames were taken at intervals of 8 min for 15 h.

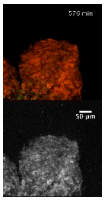

Video 7. **Inhibition of smooth neural plate morphogenesis in the absence of apoptosis.** High-magnification views of the time-lapse video of neural plate morphogenesis in *apaf-1*$^{-/-}$;*SCAT3*$^{tg/+}$ embryos, as shown in Fig. 6 B. In these embryos, D-type apoptotic cells were not observed, and both flipping of the neural ridge and bending of the neural plate were severely reduced. Caspase activation is indicated by the V/C (1.0–0.5) using pseudocolor (top). ECFP image is indicated (bottom). Live imaging was performed on an inverted confocal microscope (TCS SP5). Frames were taken at intervals of 8 min for 12 h.